One-nucleon transfer between heavy ions at intermediate energies

B. F. Bayman
School of Physics and Astronomy, University of Minnesota, Minneapolis, Minnesota

S. M. Lenzi, A. Vitturi, and F. Zardi
Dipartimento di Fisica and Istituto Nazionale di Fisica Nucleare, Padova, Italy
(Received 31 May 1994)

One-nucleon transfer processes between heavy ions at intermediate energies are studied in the framework of the eikonal distorted-wave Born approximation. Optical phase shifts describing core-core relative motion are microscopically described in the Glauber model, starting from experimental nuclear densities and nucleon-nucleon scattering amplitudes at the corresponding energies. The interaction responsible for the nucleon transfer is a complex energy-dependent potential obtained by the Abel transform of the nucleon-core phase shift. Applications to one-proton and one-neutron transfer reactions on ^{208}Pb induced by ^{12}C and ^{16}O projectiles are discussed for both angular distributions and normalization factors.

PACS number(s): 24.10.−i, 25.70.Hi

I. INTRODUCTION

The exact finite-range distorted-wave Born approximation (EFR-DWBA) has been the traditional framework for the description of one-nucleon transfer processes [1]. This has also been recently the case of ^{12}C and ^{16}O induced reactions on ^{208}Pb at intermediate energies (E/A=40–50 MeV) [2,3]. Although a good description of the shape of the angular distribution is provided by the theory, a number of questions are still under discussion. If the standard binding potential for the transferred particle is used as interaction potential, the theory overestimates the magnitudes of the cross sections by average factors of 10 and 1.3 for the ^{16}O and ^{12}C projectiles, respectively, and a comparison with the analysis of the same reactions at different energies shows that the necessary normalization factors are strongly energy dependent [2,3]. Furthermore, the use of *ad hoc* phenomenological optical parameters for the description of the distorted waves introduces an element of ambiguity into the analysis, and so it would be preferable to have a more fundamental, parameter-free approach. Finally, the high relative linear and angular momenta of the colliding nuclei require the EFR-DWBA to deal with hundreds of partial waves, which, when coupled to the nuclear channel spins, lead to a very cumbersome calculation. On the other hand, these high relative linear and angular momenta suggest that a simplified approach based on high-energy semiclassical approximations may be appropriate.

Some of these questions have been addressed by different authors. From the point of view of the ion-ion dynamics, several authors introduced time-dependent semiclassical approaches [4], where the transition probabilities are obtained by integrating proper effective transfer form factors along the classical trajectories for the relative motion. In particular, at high energies these classical trajectories reduce to simple straight lines (see, e.g., [5]). Concerning the transfer process, Dasso *et al.* [6] and Sørensen *et al.* [7] have advanced the idea that a better choice may be provided by scaling the transfer potential according to the real part of the energy-dependent optical potential used to describe nucleon-core scattering (i.e., p-^{15}N scattering in the case of proton transfer from ^{16}O) at the corresponding bombarding energy per nucleon. Calculated integrated transfer cross sections have shown the correct energy dependence.

Another possible approach to intermediate-energy heavy-ion reactions is provided by the Glauber model [8]. In a series of papers, some of the present authors have extended the Glauber model to the description of elastic and inelastic heavy-ion scattering processes (see Ref. [9] and papers therein quoted). These papers have shown the complete reliability, at these energies, of the eikonal description of the relative nucleus-nucleus motion in terms of a phase shift derived from elementary interactions and nuclear densities. These parameters have been taken from the current phenomenology with no modification or fitting procedure. In particular, there is no ambiguity associated with the choice of an optical potential.

It seems natural, therefore, to attempt to understand transfer reactions using our extended Glauber method. The model we suggest is quite simple. The transition amplitude is described by an eikonal distorted-wave approximation, where the distorted waves for the relative motion of the heavy ions are evaluated using Glauber theory. The interaction potential is taken to be the nucleon-core optical potential obtained by inverting the eikonal nucleon-core scattering phase shift at the proper energy [8].

Małecki *et al.* also have attempted to apply Glauber theory to intermediate-energy transfer reactions [10,11]. Their method is, in spirit, closer to the original Glauber work than ours, since it directly involves only nucleon-nucleon profile functions. This can only be achieved, however, under the assumption that the transfer is local-

ized in a plane perpendicular to the nuclear trajectories (at $z = 0$). The authors refer to this as the "zero longitudinal range approximation." In our opinion, this rather drastic approximation is hard to justify in terms of the geometry and dynamics of the actual nuclear reaction under consideration.

The paper is organized as follows. The formalism is presented in Sec. II. In Sec. III it is expressed in a momentum representation, which can better exploit the symmetries of the problem. Selection rules and semiclassical interpretations are discussed in Sec. IV. The application of the model to the case of transfer reactions induced by ^{12}C and ^{16}O ions on ^{208}Pb is displayed and discussed in Sec. V. Concluding remarks are given in Sec. VI.

II. THE TRANSITION AMPLITUDE

We use the conventional notation for a one-nucleon transfer reaction: $A(a,b)B$. A and b are regarded as "cores," and the nucleon c is transferred from one core to the other ($a = b + c$, $B = A + c$). The transition amplitude is written (see, e.g., Ref. [1])

$$T(\mathbf{k}_i,\mathbf{k}_f) = \int d\mathbf{r}_i\, d\mathbf{r}_f \times \Psi^{(-)*}(\mathbf{k}_f,\mathbf{r}_f) F(\mathbf{r},\mathbf{r}_c) \Psi^{(+)}(\mathbf{k}_i,\mathbf{r}_i) \ , \quad (2.1)$$

where the core-core relative vector $\mathbf{r}$ and the nucleon-light core relative vector $\mathbf{r}_c$ are related to $\mathbf{r}_i$ and $\mathbf{r}_f$ by

$$\mathbf{r}_i = \mathbf{r} + \frac{m_c}{m_a}\mathbf{r}_c, \qquad \mathbf{r}_f = \frac{m_A}{m_B}\mathbf{r} - \frac{m_c}{m_B}\mathbf{r}_c \quad (2.2)$$

(see Fig. 1). The transfer form factor is expressed by

$$F(\mathbf{r},\mathbf{r}_c) = \varphi_f^*(\mathbf{r}+\mathbf{r}_c)\ V_{bc}(\mathbf{r}_c)\ \varphi_i(\mathbf{r}_c) \ , \quad (2.3)$$

with φ_i and φ_f the initial and final bound state wave functions. The eikonal distorted waves are expressed in terms of the core (i.e., $A-b$) optical potential $V_{\rm opt}(\mathbf{b},z)$

$$\Psi^{(+)}(\mathbf{k}_i,\mathbf{r}_i) \simeq \Psi^{(+)}_{\rm eik}(\mathbf{k}_i,\mathbf{r}_i) = e^{i\mathbf{k}_i\cdot\mathbf{r}_i}\ e^{-\frac{i}{\hbar v_i}\int_{-\infty}^{z_i} dz V_{\rm opt}(\mathbf{b},z)} \ , \quad (2.4a)$$

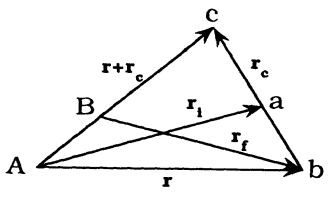

FIG. 1. Coordinates used in the transition amplitude. A and b are the cores, between which the nucleon c is transferred.

$$\Psi^{(-)*}(\mathbf{k}_f,\mathbf{r}_f) \simeq \Psi^{(-)*}_{\rm eik}(\mathbf{k}_f,\mathbf{r}_f) = e^{-i\mathbf{k}_f\cdot\mathbf{r}_f}\ e^{-\frac{i}{\hbar v_f}\int_{z_f}^{\infty} dz V_{\rm opt}(\mathbf{b},z)} \quad (2.4b)$$

Here $\mathbf{r} = \mathbf{b} + z\hat{\mathbf{z}}$, with $\hat{\mathbf{z}}$ chosen to be the direction midway between the directions of $\mathbf{k}_i$ and $\mathbf{k}_f$. From now on we assume that $V_{\rm opt}$ is axially symmetric about $\hat{\mathbf{z}}$, and thus we replace $V_{\rm opt}(\mathbf{b},z)$ with $V_{\rm opt}(b,z)$. In the cases of heavily charged systems and/or relatively low bombarding energies, where appreciable deviations from the straight-line trajectory are expected due to the Coulomb field, a first-order correction can be introduced [12] by retaining the straight-line assumption but scaling the impact parameter according to the classical Coulomb distance of closest approach.

We must distinguish between the short-range (nuclear) and the long-range (Coulomb) parts of $V_{\rm opt}$. Thus we write

$$V_{\rm opt}(b,z) = V_{\rm nuc}(b,z) + V_C(b,z) \quad (2.5)$$

and approximate the nuclear part of the core-core phase shift

$$\chi_{\rm nuc}(b) = -\frac{1}{\hbar v_i}\int_{-\infty}^{z_i} dz\ V_{\rm nuc}(b,z) - \frac{1}{\hbar v_f}\int_{z_f}^{\infty} dz\ V_{\rm nuc}(b,z) \simeq -\frac{1}{\hbar v_i}\int_{-\infty}^{\infty} dz\ V_{\rm nuc}(b,z). \quad (2.6)$$

The errors introduced by neglecting the difference between z_i and z_f and between v_i and v_f can be shown to be negligible for deflection angles of a few degrees or less, which is the angular region of experimental interest.

In the Glauber model the last integral in (2.6) can be expressed in microscopic form [13] as

$$\chi_{\rm nuc}(b) = -\frac{1}{2\pi k_{NN}}\int d\mathbf{q} e^{i\mathbf{q}\cdot\mathbf{b}} \rho_b(\mathbf{q})\rho_A(\mathbf{q}) f_{NN}(\mathbf{q}) \ , \quad (2.7)$$

where $\rho_{b,A}(\mathbf{q})$ are the two-dimensional Fourier transforms of the z-integrated ground state core densities, f_{NN} is the elementary scattering amplitude, and k_{NN} is the relative nucleon-nucleon momentum.

The approximations involved in (2.7) are not applicable to the Coulomb part of the optical potential. We thus add this part separately as

$$\chi_C(b,z) = -\frac{1}{\hbar v_i}\int_{-\infty}^{z} dz' \frac{Z_A Z_a e^2}{\sqrt{b^2+z'^2}} - \frac{1}{\hbar v_f}\int_{z}^{\infty} dz' \frac{Z_B Z_b e^2}{\sqrt{b^2+z'^2}} = -\overline{\eta}\int_{-\infty}^{\infty} \frac{dz'}{\sqrt{b^2+z'^2}} - \eta_d \int_0^z \frac{dz'}{\sqrt{b^2+z'^2}} \ , \quad (2.8)$$

with

$$\bar{\eta} = \frac{1}{2}\left(\frac{Z_A Z_a e^2}{\hbar v_i} + \frac{Z_B Z_b e^2}{\hbar v_f}\right),$$
$$\eta_d = \frac{Z_A Z_a e^2}{\hbar v_i} - \frac{Z_B Z_b e^2}{\hbar v_f}. \tag{2.9}$$

If account is taken of electronic screening at large distances, the divergent first integral in (2.8) can be replaced by $2\ln[(k_i + k_f)/2b]$, apart from an irrelevant constant. For a peripheral process such as particle transfer, the second integral in (2.8), which equals $\text{arcsinh}(z/b)$, can be approximated by z/b.

The definitions (2.2) imply that

$$\mathbf{k}_i \cdot \mathbf{r}_i - \mathbf{k}_f \cdot \mathbf{r}_f = \mathbf{q} \cdot \mathbf{r} + \mathbf{p} \cdot \mathbf{r}_c , \tag{2.10}$$

with

$$\mathbf{q} = \mathbf{k}_i - \frac{m_A}{m_B}\mathbf{k}_f , \qquad \mathbf{p} = \frac{m_c}{m_a}\mathbf{k}_i + \frac{m_c}{m_B}\mathbf{k}_f. \tag{2.11}$$

If we combine (2.10) with the work of the previous paragraphs, the transfer amplitude (2.1) becomes

$$T(\mathbf{k}_i, \mathbf{k}_f) = \int d\mathbf{r}\, d\mathbf{r}_c\, e^{(i\mathbf{q}\cdot\mathbf{r} + \mathbf{p}\cdot\mathbf{r}_c) i\chi(\mathbf{b},z)} \varphi_f^*(\mathbf{r} + \mathbf{r}_c) \times V_{bc}(\mathbf{r}_c)\, \varphi_i(\mathbf{r}_c) \tag{2.12}$$

with

$$\chi(b,z) = \chi_{\text{nuc}}(b) - 2\bar{\eta} \ln\left(\frac{k_i + k_f}{2b}\right) - \eta_d \frac{z}{b} , \tag{2.13}$$

and with χ_{nuc} given by (2.7).

The complex, energy-dependent transfer potential $V_{bc}(\mathbf{r}_c)$ is evaluated by applying an Abel transform

$$V_{bc}(r) = \frac{\hbar v_{bc}}{\pi r}\frac{d}{dr}\int_r^\infty \frac{\chi_{bc}(b)}{(b^2 - r^2)^{1/2}}\, b\, db , \tag{2.14}$$

to the nucleon-core phase shift $\chi_{bc}(b)$, which is constructed by using (2.7) without the factor $\rho_A(\mathbf{q})$ in the integrand.

It is of interest to compare our formalism with semiclassical time-dependent approaches. To do this, we rewrite Eq. (2.12) as

$$T(\mathbf{k}_i, \mathbf{k}_f) = \int d\mathbf{b}\; e^{i\mathbf{q}_\perp \cdot \mathbf{b}} e^{i\chi(\mathbf{b})} \tau_{i,f}(\mathbf{b}) \tag{2.15}$$

where

$$\tau_{i,f}(\mathbf{b}) = \int dz\, e^{iq_z z} e^{-\frac{i}{\hbar v}\frac{Z_c(Z_A - Z_b)e^2}{b} z} \times \int d\mathbf{r}_c \varphi_f^*(\mathbf{r} + \mathbf{r}_c)\, V_{bc}(\mathbf{r}_c)\, \varphi_i(\mathbf{r}_c)\, e^{i\mathbf{p}\cdot\mathbf{r}_c}. \tag{2.16}$$

To leading order in the ratios between excitation energy and total kinetic energy and between transferred mass and total mass, one gets

$$q_z \simeq -\frac{Q}{\hbar v} - \tfrac{1}{2} m_c v. \tag{2.17}$$

In the present approach based on the straight-line approximation, the integral over z can be directly transformed into an integral over t ($z = vt$) leading to

$$q_z z = -\frac{t}{\hbar}(Q + \tfrac{1}{2} m_c v^2), \tag{2.18}$$

which coincides, for example, with the corresponding term in Ref. [14].

III. EVALUATION OF THE TRANSITION AMPLITUDE

To simplify the notation, we will at first ignore intrinsic spin. The structure of the integrals appearing in Eq. (2.12) suggests that it is convenient to work in momentum space [15]. We express therefore the quantities appearing in this equation in terms of their Fourier transforms:

$$V_{bc}(\mathbf{r}_c)\, \varphi_i(\mathbf{r}_c) = \frac{1}{(2\pi)^{3/2}} \int d\mathbf{w}\, e^{i\mathbf{r}_c \cdot \mathbf{w}}\, \psi_i(\mathbf{w}), \tag{3.1a}$$

$$\varphi_f(\mathbf{r} + \mathbf{r}_c) = \frac{1}{(2\pi)^{3/2}} \int d\mathbf{w}\, e^{i(\mathbf{r}+\mathbf{r}_c)\cdot \mathbf{w}}\, \psi_f(\mathbf{w}), \tag{3.1b}$$

$$e^{-i\chi(\mathbf{r})} = \frac{1}{(2\pi)^{3/2}} \int d\mathbf{w}\, e^{i\mathbf{r}\cdot\mathbf{w}}\, \psi_\chi(\mathbf{w}). \tag{3.1c}$$

If these are inserted into (2.12), the $\mathbf{r}$ and $\mathbf{r}_c$ integrals can be performed immediately, with the result

$$T(\mathbf{k}_i, \mathbf{k}_f) = (2\pi)^{3/2} \int d\mathbf{w}\, \psi_f^*(\mathbf{w}) \psi_\chi(\mathbf{w} - \mathbf{q}) \times \psi_i(\mathbf{w} - \mathbf{p}). \tag{3.2}$$

The structure of (2.13) suggests that we work in cylindrical coordinates

$$\begin{aligned} T(\mathbf{k}_i, \mathbf{k}_f) &= (2\pi)^{3/2} \int d\mathbf{w}_\perp\, dw_z\, \psi_f^*(\mathbf{w}_\perp, w_z) \psi_\chi(\mathbf{w}_\perp - \mathbf{q}_\perp, w_z - q_z) \psi_i(\mathbf{w}_\perp - \mathbf{p}_\perp, w_z - p_z) \\ &= (2\pi)^2 \int d\mathbf{w}_\perp \int_0^\infty b\, db\, J_0(|\mathbf{w}_\perp - \mathbf{q}_\perp| b)\, e^{i[\chi_{\text{nuc}}(b) - 2\bar{\eta}\, \ln(\frac{k_i + k_f}{2b})]} \\ &\quad \times \psi_f^*(\mathbf{w}_\perp, q_z - \eta_d/b) \psi_i(\mathbf{w}_\perp - \mathbf{p}_\perp, q_z - p_z - \eta_d/b). \end{aligned} \tag{3.3}$$

To disentangle the dependence on $\mathbf{w}_\perp$ and b in (3.3), we keep only the first two terms in an expansion of $\psi_f^*\psi_i$ around the grazing value b=11 fm ($\equiv b_0$), i.e. the value at the center of the most important region of impact parameter space:

$$\psi_f^*(\mathbf{w}_\perp, q_z - \eta_d/b)\psi_i(\mathbf{w}_\perp - \mathbf{p}_\perp, q_z - p_z - \eta_d/b)$$

$$\simeq \psi_f^*(\mathbf{w}_\perp, q_z - \eta_d/b_0)\psi_i(\mathbf{w}_\perp - \mathbf{p}_\perp, q_z - p_z - \eta_d/b_0) + (b - b_0)\frac{d}{db}\psi_f^*(\mathbf{w}_\perp, q_z - \eta_d/b)\psi_i(\mathbf{w}_\perp - \mathbf{p}_\perp, q_z - p_z - \eta_d/b)_{b=b_0}. \tag{3.4}$$

This enables us to write (3.3) in the following more convenient form:

$$T(\mathbf{k}_i, \mathbf{k}_f) = (2\pi)^2\Big[\int d\mathbf{w}_\perp\ \psi_f^*(\mathbf{w}_\perp, q_z - \eta_d/b_0)\psi_i(\mathbf{w}_\perp - \mathbf{p}_\perp, q_z - p_z - \eta_d/b_0)\ F_0(|\mathbf{w}_\perp - \mathbf{q}_\perp|)$$
$$+ \int d\mathbf{w}_\perp\ \frac{d}{db}\psi_f^*(\mathbf{w}_\perp, q_z - \eta_d/b)\psi_i(\mathbf{w}_\perp - \mathbf{p}_\perp, q_z - p_z - \eta_d/b)_{b=b_0}\ F_1(|\mathbf{w}_\perp - \mathbf{q}_\perp|)\Big], \tag{3.5}$$

with

$$F_0(|\mathbf{w}_\perp - \mathbf{q}_\perp|) = \int_0^\infty b\ db\ J_0(|\mathbf{w}_\perp - \mathbf{q}_\perp|b) \times e^{i[\chi_{\rm nuc}(b) - 2\bar{\eta}\ \ln(\frac{k_i + k_f}{2b})]}, \tag{3.6a}$$

$$F_1(|\mathbf{w}_\perp - \mathbf{q}_\perp|) = \int_0^\infty b\ db\ (b - b_0)\ J_0(|\mathbf{w}_\perp - \mathbf{q}_\perp|b) \times e^{i[\chi_{\rm nuc}(b) - 2\bar{\eta}\ \ln(\frac{k_i + k_f}{2b})]}. \tag{3.6b}$$

The one- and two-dimensional integrals in (3.5), (3.6a), and (3.6b) were evaluated numerically. This was facilitated by first expanding $V_{bc}(r)\varphi_i(\mathbf{r})$ and $\varphi_f(\mathbf{r})$ in terms of eigenfunctions of three-dimensional harmonic oscillator potentials. The operations of transforming from spherical polar to cylindrical coordinates, performing Fourier transforms, and differentiating with respect to b, could be done analytically due to the convenient properties of harmonic oscillator eigenstates.

The second term in (3.5) depends on the quantity η_d defined in Eq. (2.9), the difference between the Sommerfeld parameters in the initial and final channels. It is significant only in the case of proton transfer, where it has the effect of increasing the transfer cross section. For example, in the ^{208}Pb(^{16}O,^{15}N)^{209}Bi reaction, the Coulomb repulsion between ^{208}Pb and ^{16}O slows down the approaching nuclei more effectively than the weaker Coulomb repulsion between ^{209}Bi and ^{15}N accelerates the separating nuclei. This decreases the longitudinal linear momentum mismatch experienced by the proton transferred from ^{16}O to ^{209}Bi, and thus increases the transfer cross section.

IV. MAGNETIC QUANTUM NUMBERS AND INTRINSIC SPIN

We have so far designated the initial and final bound state wave functions by φ_i and φ_f. Now let us introduce orbital angular momentum quantum numbers $(\varphi_{m_i}^{l_i}, \varphi_{m_f}^{l_f})$. Correspondingly, the notation for the transfer amplitude should also include the initial and final m values: $T(\mathbf{k}_i, l_i\ m_i; \mathbf{k}_f, l_f\ m_f)$. The physical interpretation is clearest when the quantization direction for m_i and m_f is chosen to be perpendicular to the reaction plane, in the same direction as the relative orbital angular momentum vector. In Fig. 2 this is taken to be the $+\hat{\mathbf{y}}$ axis.

When the nucleon is transferred between the two cores, the z component of its linear momentum changes. With projectile energies of 40–50 MeV per nucleon, this change can exceed the modest impulse that can be supplied by the transfer potential. This large linear momentum mismatch is an indication that the corresponding transfer will be inhibited. From Fig. 2(a) which illustrates transfer occurring while the nuclei pass each other on (repulsive) Coulomb-dominated trajectories, one can infer [16] that the condition of small mismatch in p_z (and thus in velocity component v_z) is approximately

$$\frac{m_c k}{\mu_{Ab}} \simeq \frac{M_i}{r_i} + \frac{M_f}{r_f}. \tag{4.1}$$

Here M_i and M_f are the projections, on the $+\hat{\mathbf{y}}$ axis, of the initial and final single-particle orbital angular momenta of the transferred nucleon, and r_i and r_f are the radii of the orbits around the two cores. For 793 MeV ^{16}O projectiles on a ^{208}Pb target, $m_c k/\mu_{Ab} \simeq 1.6$ fm^{-1}, r_i=3 fm, r_f=7 fm. If we assume that the nucleon came from the p orbit, then $|M_i| \leq 1$. Also $|M_f| \leq l_f$, which is 7 for a $j_{15/2}$ orbit. Thus we get the closest approximation to the momentum matching condition

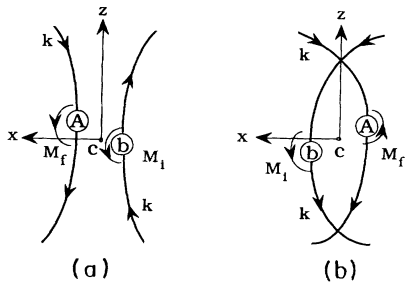

FIG. 2. (a) Nucleon c is transferred as the cores move past each other on the Coulomb-dominated trajectories. (b) The deflection angle is the same as in (a), but the attractive part of the core-core interaction dominates the trajectory.

$$1.6\ \text{fm}^{-1} \simeq \frac{M_i}{3\ \text{fm}} + \frac{M_f}{7\ \text{fm}} \tag{4.2}$$

by choosing M_i and M_f to be as large as possible ($M_i = l_i$, $M_f = l_f$). On the other hand, if the transfer occurs when the cores pass each other on orbits dominated by the attractive part of the core-core interaction, the condition for small mismatch in p_z is approximately

$$\frac{m_c k}{\mu_{Ab}} \simeq -\left[\frac{M_i}{r_i} + \frac{M_f}{r_f}\right], \tag{4.3}$$

which is most closely achieved by setting $M_i = -l_i, M_f = -l_f$.

Table I shows partial differential cross sections for different M_i, M_f combinations for neutron transfer from the $0p$ orbit in ^{12}C to the $1g$ orbit in ^{209}Pb. The deflection angle is 4°. Notice that the largest contribution comes from $M_i = l_i, M_f = l_f$, corresponding to the Coulomb-dominated orbit of Fig. 2(a). The table only has entries for odd values of $M_i - M_f$, since the reflection symmetry across the plane of the orbit guarantees that T will be zero unless $(-1)^{M_i - M_f} = \Pi_i \Pi_f$ (Bohr's theorem).

Since the "near-side" and "far-side" [1] orbits with the same deflection angle, shown in Fig. 2, are associated with different (M_i, M_f) values, we do not expect there to be significant interference between contributions from these orbits in the transfer matrix element. Thus the angular distributions do not show the forward-angle fine-structure oscillations that would be associated with this interference.

TABLE I. $|T(\mathbf{k}_i, 1, M_i; \mathbf{k}_f, 4, M_f)|^2$ for transfer of a neutron from the $0p$ shell of ^{12}C to the $1g$ shell of ^{209}Pb. The ^{12}C kinetic energy is 480 MeV, and the deflection angle is 4°.

M_i	M_f	$\lvert T(\mathbf{k}_i, 1, M_i; \mathbf{k}_f, 4, M_f)\rvert^2$
−1	−4	59.2
−1	−2	4.9
−1	0	1.6
−1	2	5.7
−1	4	51.5
0	−3	3.3
0	−1	0.2
0	1	2.7
0	3	21.8
1	−4	9.6
1	−2	2.3
1	0	1.7
1	2	23.4
1	4	555.3

To express the transition matrix element in terms of single-particle states for which j is a good quantum number, we must make an assumption about the role of intrinsic spin in the transfer process. We will make the simplest assumption, namely, that it has no role, except for the effect of the spin-orbit potential on the single-particle radial functions. Thus we assume no spin flip during the transition, and no dependence of the transition amplitude on spin direction:

$$\begin{aligned} &T(\mathbf{k}_i, l_i\ j_i\ M_i; \mathbf{k}_f, l_f\ j_f\ M_f) \\ &= (l_i\ \tfrac{1}{2}\ M_i + \tfrac{1}{2}\ -\tfrac{1}{2} | j_i\ M_i)\ (l_f\ \tfrac{1}{2}\ M_f + \tfrac{1}{2}\ -\tfrac{1}{2} | j_f\ M_f)\ T(\mathbf{k}_i, l_i\ M_i + \tfrac{1}{2}; \mathbf{k}_f,\ l_f\ M_f + \tfrac{1}{2}) \\ &\quad + (l_i\ \tfrac{1}{2}\ M_i - \tfrac{1}{2}\ \tfrac{1}{2} | j_i\ M_i)\ (l_f\ \tfrac{1}{2}\ M_f - \tfrac{1}{2}\ \tfrac{1}{2} | j_f\ M_f)\ T(\mathbf{k}_i, l_i\ M_i - \tfrac{1}{2}\ ; \mathbf{k}_f, l_f\ M_f - \tfrac{1}{2}) \end{aligned} \tag{4.4}$$

The $M_i \pm \frac{1}{2}$, $M_f \pm \frac{1}{2}$ on the right-hand side of (18) are the $\hat{\mathbf{y}}$ components of the single-particle orbital angular momenta. The comments made previously about the reflection symmetry of the transition amplitude, and the dominant role played by the transitions between states of maximum M_i and M_f, also apply to $T(\mathbf{k}_i, l_i\ j_i\ M_i; \mathbf{k}_f, l_f\ j_f\ M_f)$.

The parameters of the bound state wells are given in Tables II and III. They are the same as those used by Mermaz *et al.* [2,3]. The standard separation energy prescription has been used, in which the well depth is varied to achieve a single-nucleon binding energy equal to the separation energy of each nucleon state.

V. ANGULAR DISTRIBUTIONS AND SPECTROSCOPIC FACTORS

Figure 3 shows a comparison of our calculated angular distributions (solid lines) with the experimental data of Refs. [2,3] for single-nucleon transfer onto a ^{208}Pb target, from projectiles of 480 MeV ^{12}C and 793 MeV ^{16}O. Each

TABLE II. Bound state well parameters; the depth of the central potential is given in Table III for each individual level.

Nucleus	r_0 (fm)	a_0 (fm)	r_c (fm)	r_{so} (fm)	a_{so} (fm)	V_{so} (MeV)
^{12}C,^{16}O	1.20	0.65	1.2	1.2	0.65	7.0
^{209}Bi	1.28	0.76	1.2	1.09	0.6	6.0
^{209}Pb	1.25	0.63	1.2	1.09	0.5	7.0

calculated curve has been multiplied by a scale factor S_j to produce the best visual fit to the data. Apart from this scale factor, there are no adjustable parameters in the theory. Everything we need is defined in terms of measured nuclear density distributions and nucleon-nucleon transition amplitudes. In particular, we have not had to choose or vary any parameters of optical potentials. Thus the generally good agreement between the shapes of the calculated angular distributions and the experimental data supports the validity of the application of this Glauber-like method to single-nucleon transfer, with projectile energy in the range of $40A$–$50A$ MeV.

Table IV shows the S factors used to normalize the calculated differential cross sections, to yield the fits shown in Fig. 3. When account is taken of the error bars on the experimental data points, and the ambiguities introduced by the lack of perfect agreement between the shapes of

TABLE III. The central well depth V required to obtain the observed single-nucleon (π: proton, ν: neutron) separation energy (SE).

Nucleus	State	E^* (MeV)	SE (MeV)	V (MeV)
^{12}C	$0p_{3/2}$ (π)	0	15.95	67.13
	$0p_{3/2}$ (ν)	0	18.72	66.59
^{16}O	$0p_{1/2}$ (π)	0	12.12	61.19
	$0p_{1/2}$ (ν)	0	15.66	60.52
^{209}Bi	$1f_{5/2}$ (π)	2.82	0.97	59.56
	$1f_{7/2}$ (π)	0.90	2.89	59.53
	$0h_{9/2}$ (π)	0	3.79	59.92
	$0i_{13/2}$ (π)	1.61	2.18	59.21
^{209}Pb	$1g_{7/2}$ (ν)	2.49	1.44	46.23
	$1g_{9/2}$ (ν)	0	3.93	46.11
	$0i_{11/2}$ (ν)	0.78	3.15	47.25
	$0j_{15/2}$ (ν)	1.42	2.51	44.70

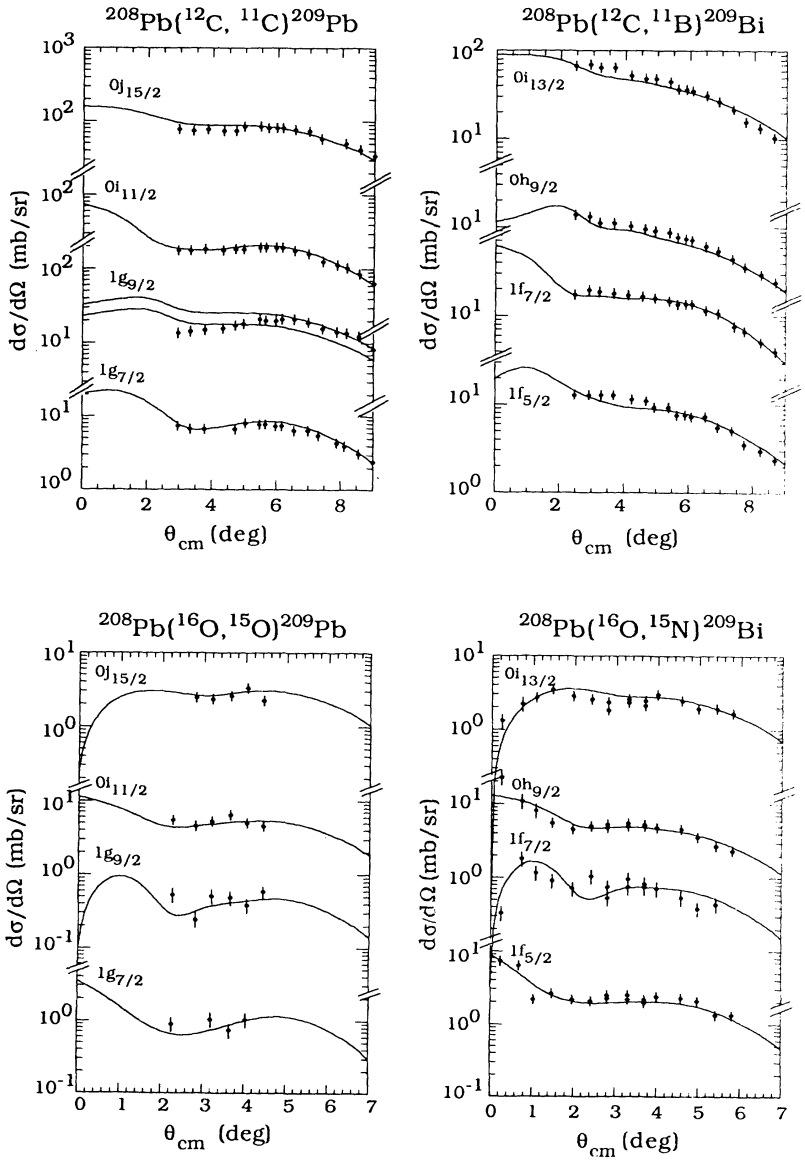

FIG. 3. Angular distributions obtained for single-neutron and single-proton transfer onto a ^{208}Pb target, from projectiles of 480 MeV ^{12}C and 793 MeV ^{16}O. The different final single-particle states are given for each curve. The experimental data are taken from Refs. [2,3]. Each calculated curve has been multiplied by a scale factor S_j, whose values are given in Table IV.

TABLE IV. S is the factor by which the calculated cross sections from and to pure single-particle states must be multiplied in order to produce the degree of agreement with the data shown in Fig. 3. The "theory" columns show calculated spectroscopic factors [17] for transfer between ^{208}Pb and ^{209}Pb or ^{209}Bi.

Final state in ^{209}Bi	E^* (MeV)	S (^{16}O,^{15}N)	S (^{12}C,^{11}B)	S (^{209}Bi) (theory)
$9/2^-$	0	0.33	0.50	0.95
$7/2^-$	0.90	0.33	0.75	0.85
$13/2^+$	1.61	0.33	0.67	0.70
$5/2^-$	2.82	0.30	1.40	0.66
Final state in ^{209}Pb	E^* (MeV)	S (^{16}O,^{15}O)	S (^{12}C,^{11}C)	S (^{209}Pb) (theory)
$9/2^+$	0	0.25	0.7–1.0	0.89
$11/2^+$	0.78	0.20	1.6	0.96
$15/2^-$	1.42	0.20	1.0	0.62
$7/2^+$	2.49	0.28	2.8	0.84

the calculated and experimental differential cross section curves, an uncertainty of about ±10% should be attributed to each S value in Table IV, except in the case of ^{208}Pb(^{12}C,^{11}C) ^{209}Pb($9/2^+$), where the uncertainty is about 30%.

The ratio of experimental and DWBA cross sections should equal the product of two spectroscopic factors, one for nucleon pickup from the ^{12}C or ^{16}O projectile, and one for nucleon stripping to the ^{208}Pb target. In order to focus attention on the ^{208}Pb spectroscopic factor, let us assume that the ground states of the relevant light nuclei are perfectly described by the j-j coupling shell model. This implies spectroscopic factors of 2 for (^{16}O,^{15}N$_{1/2^-}$) and (^{16}O,^{15}O$_{1/2^-}$) and 4 for (^{12}C,^{11}B$_{3/2^-}$) and (^{12}C,^{11}C$_{3/2^-}$). These light-particle spectroscopic factors are included in the calculated cross sections used to determine the ratios S_j presented in Table IV. Ideally, then, the S_j should equal the spectroscopic factor for proton and neutron addition to ^{208}Pb. Theoretical values [17] for these spectroscopic factors are also listed in Table IV. It is seen that for the (^{16}O,^{15}N) reaction, our S_j values are about 2 – 3 times smaller than the theoretical ^{208}Pb→^{209}Bi spectroscopic factors. For the (^{16}O,^{15}O) reaction, the corresponding discrepancy is about 3 – 5. These are the factors by which our transfer calculation, combined with the theoretical spectroscopic factors, would overestimate the measured cross sections. Mermaz *et al.* report a similar normalization discrepancy when they fit their data using a DWBA calculation. In their case, the discrepancy factor is between 5 and 10, depending upon the optical parameters used in the DWBA calculation.

Whereas the $0p_{1/2}$ shell is very nearly full in the ^{16}O ground state, it is probably a poor assumption to assign a filled $0p_{3/2}$ shell to the ^{12}C ground state. Thus a comparison of ^{208}Pb(^{12}C,^{11}B$_{3/2^-}$)^{209}Bi and ^{208}Pb(^{12}C, ^{11}C$_{3/2^-}$)^{209}Bi S_j factors with theoretical ^{208}Pb→^{209}Bi and ^{208}Pb →^{209}Pb spectroscopic factors is probably less meaningful than for ^{16}O projectiles. In fact the ^{12}C ground state is probably strongly deformed, and inelastic coupling to other channels might affect the nucleon transfer cross sections. It is seen from Table IV, however, that the simple approximation of transfer from a filled $0p_{3/2}$ shell reproduces the observed cross sections within a factor of 2, except in the cases of transfer to the $5/2^-$ state of ^{209}Bi and the $7/2^+$ of ^{209}Pb. These two cases present the worst examples of linear momentum mismatch of the transferred nucleon. Our model does not have a mechanism to supply the required impulse.

VI. CONCLUDING REMARKS

Glauber-like methods, based on the straight-line eikonal approximation, have their natural sphere of applications in the description of elastic and inelastic processes at intermediate and high energy. The literature of the successes obtained in these applications to particle, nuclear, and chemical physics is magnificent. The present work is an exploration of the boundaries of applicability of the method in situations in which a mass transfer causes a sudden discontinuity of the trajectories. We find that the shapes of the predicted angular distributions are in good accord with the experimental data, and are similar to those given by the EFR-DWBA. The absolute magnitudes of the differential cross sections are somewhat closer to the data than those of the EFR-DWBA. Moreover, this measure of agreement has been achieved by a parameter-free description. We believe that this gives the Glauber approach a significant conceptual, and practical, advantage over the EFR-DWBA.

ACKNOWLEDGMENTS

One of us (BFB) wishes to express his appreciation to the Minnesota Supercomputer Institute for a grant that facilitated some of these computations. He also acknowledges financial support from the Italian Institute for Nuclear Physics (INFN).

[1] G. R. Satchler, *Direct Nuclear Reactions* (Clarendon Press, Oxford, 1983).
[2] M. C. Mermaz *et al.*, Z. Phys. A **326**, 353 (1987).
[3] M. C. Mermaz *et al.*, Phys. Rev. C **37**, 1942 (1988).
[4] R. A. Broglia and A. Winther, *Heavy ion reactions* (Addison-Wesley, Reading, MA, 1991).
[5] A. Bonnacorso, D. M. Brink, and L. Lo Monaco, J. Phys. G **13**, 1407 (1987).
[6] C. H. Dasso, S. Landowne and H. H. Wolter, Nuovo Cimento A **92**, 50 (1986).
[7] J. H. Sørensen, A. Winther, and G. Pollarolo, Phys. Lett. B **225**, 41 (1989); Nucl. Phys. **A522**, 578 (1991).
[8] R. J. Glauber, *High-energy collisions theory, Lectures in Theoretical Physics* (Interscience, New York, 1959), p.

315.
[9] F. Zardi, S. M. Lenzi, and A. Vitturi, Phys. Rev. C **49**, 1635 (1994).
[10] A. Małecki, J. Phys. (Paris) **39**, 1049 (1978).
[11] A. Małecki, B. Minetti, G. Rosa, P. Di Giacomo, and A. Reale, Nuovo Cimento A **63**, 321 (1981).
[12] A. Vitturi and F. Zardi, Phys. Rev. C **36**, 1404 (1987).
[13] W. Czyż and L. C. Maximon, Ann. Phys. (N.Y.) **52**, 59 (1969).
[14] H. Hasan and D. M. Brink, J. Phys. G **4**, 1573 (1978).
[15] W. von Oertzen, Phys. Lett. **115B**, 95 (1985).
[16] D. M. Brink, Phys. Lett. **40B**, 37 (1972).
[17] P. Ring and E. Warner, Nucl. Phys. **A211**, 198 (1973).